Frontiers in Scientific Research and Technology

Online ISSN: 2682-297
Print ISSN: 2682-2962
http://fsrt.journals.ekb.eg

FSRT J 1 (2020) 1-7 DOI: 10.21608/fsrt.2019.18419.1000

Characterization and optical properties of annealed ZnO nanoparticles prepared by microwave irradiation

M. M. El-Desoky [a]*, M. A. Ali [a], G. Afifi [b], H. Imam [b]

[a] *Department of Physics, Faculty of Science, Suez University, Suez, Egypt*
[b] *National Institute of Laser Enhanced Sciences, Cairo University, Egypt.*

ARTICLE INFO

Article history:
Received 2 November 2019
Received in revised form 16 November 2019
Accepted 16 November 2019
Available online 16 November 2019

Keywords
Nanostructures,
ZnO,
Microwave,
Optical properties

ABSTRACT

Annealed ZnO nanoparticles at 300, 350, 400, 450 and 500 oC in air were prepared by microwave method. The effects of annealing temperature on the structural and optical properties of annealed ZnO nanoparticles by XRD, transmittance spectra, and photoluminescence (PL) were investigated. The XRD reveal the presence of hexagonal wurtzite structure of ZnO and average grain size was obtained to be between 25.7–36.4nm. From the UV-Vis spectra the vacancy energy level was determined and the effect of annealing temperature on the energy level is illustrated. The vacancy energy level of ZnO was found to be 2.25 - 2.37 eV. The PL spectra show that all the samples emits strong UV and very weak violet, blue and green emissions this refers to the high crystal quality of annealed ZnO nanoparticles.

1. Introduction

Zinc oxide is an exclusive and important inorganic material that has attracted wide research due to its characteristic features and new applications in wide areas of science and technology. It has many properties like semiconducting, pyroelectric, optoelectronics, catalysis and piezoelectric [1,2]. The absence of center of symmetry in the wurtuzite structure of ZnO finds its use as piezoelectric devices [3]. ZnO is a large band gap n-type semiconductor (3.37 eV) with large exciton binding energy of 60 meV at room temperature. This property has made ZnO as one of the most smart photocatalyst in the treatment of wastes and contaminants present in air and water by photo degradation mechanism. As the photocatalyst reaches the nanoscale, the photogenerated electron–hole pair combination decreases due to the fast photocatalytic reaction at the surface of the catalyst [4–5].

However, the optical properties of ZnO nanoparticles show a significant role in photochemical properties. In the latest years, many researchers have used different preparative techniques like hydrothermal route, sol–gel process, and pulsed laser deposition, for the preparation of zinc oxide nanoparticles with different morphologies [6–7].

Microwave irradiation as a heating method has found a number of applications in chemistry. The operations of microwave irradiation in the preparation of nanoparticles have been specified in latest years [8]. Compared to the conventional approaches, the microwave synthesis has the advantages of manufacturing small particle size with high purity due to short reaction time. Some investigators have studied the effects of annealing temperature many properties of ZnO nanoparticles by sol-gel method. In these papers, most ZnO nanoparticles were synthesis by sol-gel route and the annealing temperature is generally higher than 600^{o}C [9–10]. The effect of annealing temperature on the structural and optical properties of ZnO nanoparticles is rarely studied. In this paper ZnO nanoparticles were synthesis using microwave route and then were annealed in air at 300, 350, 400, 450 and 500^{o}C.The structural and optical properties of the annealed ZnO nanoparticles are studied using X-ray diffraction (XRD), UV–Visible-Near IR Spectroscopy and photoluminescence (PL) spectroscopy measurements. The structural and optical properties study reveals important differences in these properties of the nanoparticles with respect to annealing temperature.

2. Materials and methods

All elements were obtained from Sigma Aldrich. In a typical process, 5gm zinc nitrate hexahydrate (Zn $(NO_3)2{\cdot}6H_2O$) (99.99%) was dissolved into 30mL distillated water. After stirring for several minutes, aqueous solution of 5 mole sodium hydroxide was gradually added to the

* Corresponding authors at: Suez University
E-mail addresses: mmdesoky@suezuniv.edu.eg (M. M. El-Desoky)

reaction mixture. It was then stirred for 20 minutes. Finally, the mixture was located in microwave irradiation for 3 minutes. The white solid product was washed with distilled water and dried in air at 80°C.

The prepared ZnO nanoparticles at room temperature (RT) were subjected to annealing treatment in air for 2 h at temperatures of 300, 350, 400 ,450 and 500 ^{0}C that denoted by Zn_{300}, Zn_{350}, Zn_{400}, Zn_{450}, Zn_{500} respectively. The prepared samples at room temperature were denoted by Zn_{RT}.

X-ray diffraction (XRD) patterns were studied in order to find the structure and the crystal size of the prepared samples by using XPERT-PRO-PANalytical-Nertherland (with Cu-K_α radiation). The diffraction data were recorded for 2θ between 20° and 80° with a resolution of 0.02°. The optical transmittance properties of ZnO samples were measured by using PG instruments Ltd-T80+UV/vis spectrometer in the spectral range of 200–850 nm. The photoluminescence (PL) measurements were performed using PerkinElmer-Ls55 Fluorescence spectrometer with Xenon lamp as the excitation source.

3. Result and Discussion

3.1 XRD

The XRD pattern of annealed ZnO nanoparticles is shown in Fig (1) at different temperature. The patterns shows that all samples have (100), (002), (101), (102), (110), (103), (200), (112), (201), (004) and (202) peaks. This means that the present samples are identical to the hexagonal phase with Wurtzite structure. This diffraction peaks mean the nanocrystalline nature which agreement with the JCPDS card no.04-015-0825.

The average grain sizes (D) of annealed ZnO nanoparticles were evaluated due to Sherrer's equation [11]:

$$D = \frac{k\lambda}{\beta \cos\theta} \qquad (1)$$

Where θ is the Bragg angle of the X-ray diffraction peak, k ~ 1, λ=0.15406 nm, λ is the wavelength of Cu(Kα) radiation, and β represents the corrected experimental full-width at half-maximum of the diffraction peak in units of radians. The average grain sizes (D) of present samples are shown in Fig (1) as a function of the annealing temperature and listed in Table (1).

As shown in Fig (2), The grain size increases from 25.7nm to 36.4nm as the annealing temperature increases from RT to 450^{0}C then from 450^{0}C to 500^{0}C the grain size decreases from 36.4nm to 33nm, this result can be clarified by the two causes: At first, atomic mobility increases with annealing temperature, improving the capability of atoms to find the most energetically favored sites. At second, the densities of the crystallographic defects containing dislocations, interstitials and vacancies ZnO nanoparticles decrease quickly with increasing the annealing temperature [12].

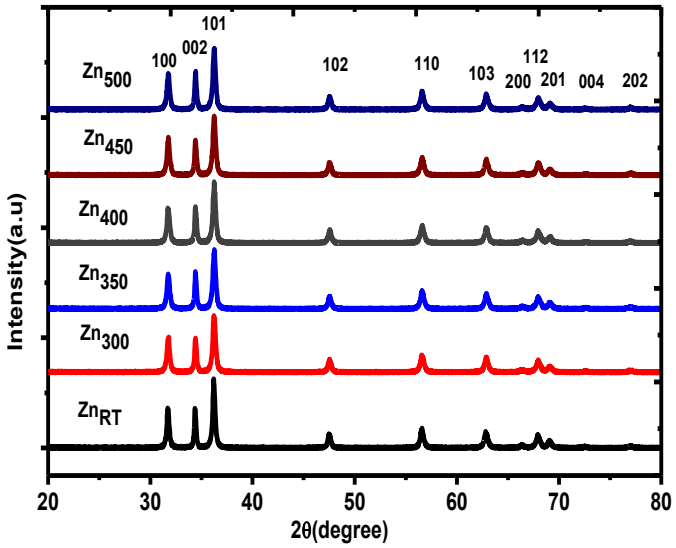

Fig (1): XRD pattern of ZnO nanoparticles annealed at different temperatures.

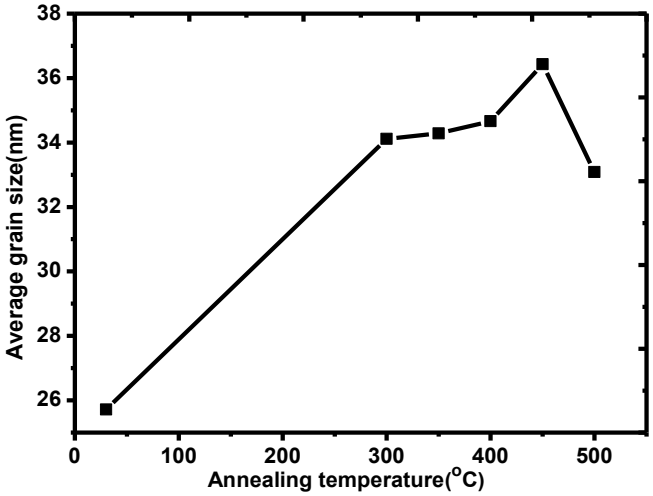

Fig (2): The average grain size of ZnO nanoparticles as a function of annealing temperature.

It is well known that ZnO has hexagonal unit cell with two lattice parameters (a) and (c) that can be calculated from the XRD pattern by using the following equations [12,13]:

$$\frac{1}{d^2} = \frac{4}{3}\left(\frac{h^2+k^2+hk}{a^2}\right) + \frac{l^2}{c^2} \qquad (2)$$

$$c = \frac{\lambda}{\sin\theta_{002}} \quad \text{and} \quad a = \frac{\lambda}{\sqrt{3}\sin\theta_{100}} \qquad (3)$$

Where θ_{100} and θ_{002} are the diffraction angles of the peaks (100) and (002) ,respectively and "d" is the interplanar spacing. The values of "c" and "a" parameters of annealed ZnO nanoparticles are listed in Table (1).

Table (1): Lattice parameters, Grain size and Density at different annealing temperatures.

Annealing temperature (^{o}C)	$2\theta_{002}$	$2\theta_{100}$	C(^{o}A)	a(^{o}A)	Density (g/cm^3)	Grain size(nm)
RT	34.389	31.719	5.209	3.253	5.661	25.7
300	34.429	31.758	5.203	3.249	5.680	34.1
350	34.431	31.760	5.203	3.249	5.681	34.2
400	34.423	31.744	5.204	3.251	5.675	34.6
450	34.425	31.760	5.204	3.249	5.681	36.4
500	34.429	31.759	5.203	3.249	5.681	33

The density (ρ) of annealed ZnO nanoparticles were calculated by using the following formula[12]:

$$\rho = \frac{nM}{VNa} \quad (4)$$

Where n=6 is the number of atoms per unit cell, M=81.408 g/mol is the molecular weight, V= $\frac{3\sqrt{3}}{2}$ a^2c is the cell volume in cm^3, N_a =0.60225 x10^{24} mol^{-1} is Avogadro's number. The density values of annealed ZnO nanoparticles (ρ) in g/cm^3 are listed in Table (1).

The location of (002) diffraction peak for annealed ZnO nanoparticles at RT, 300, 350, 400,450 and 500^{0}C seem at 34.389, 34.429, 34.431,34.423,34.425 and 34.429 ,respectively as listed in Table 1 . Compared with the (002) peak position of ZnO powder (2θ = 34.432), the diffraction angle of all annealed ZnO nanoparticles decrease in comparison with bulk ZnO, which results in the increase of interplanar spacing and c-axis values, and the decrease of the density of annealed ZnO nanoparticles[14].

3.2. Optical properties

The Transmittance spectrum of ZnO nanoparticles annealed at different temperatures is shown in Fig.(3). It is observed that all the annealed ZnO nanoparticles have the same absorption band at wavelength 377nm. The optical band gap E_g can be estimated by using Tauc's law [15]:

$$\alpha h\upsilon = \beta (h\upsilon - E_g)^{n} \quad (5)$$

Where E_g is the band gap agreeing to a specific transition occurring in the film, β is a band edge constant, υ is the transition frequency and the exponent n symbolizes the nature of band transition. n = 1/2 and 3/2 agrees to direct allowed and direct forbidden transitions and n = 2 and 3 agrees to indirect allowed and indirect forbidden transitions, respectively. The optical band gap E_g can then be found from the intercept of $(\alpha h\upsilon)^2$ vs. hυ for direct transitions. It is showed that for present films the best straight line is found for n =1/2 which is predictable for direct allowed transition as shown in Fig (4).

The optical band gap decreases from 2.37 eV to 2.29 eV as the annealing temperature increase from RT to 500^{o}C, and the values E_g are listed in Table (2). It is known that the bulk ZnO has an optical band gap at 3.30 eV. The values of the optical band gap E_g of annealed ZnO nanoparticles are too low to be an indication of the band gap energies but rather an indication of the vacancy energy levels (E_v). This shows that an increase in the annealing temperature decreased the vacancy energy level. The decrease in the vacancy energy levels of annealed ZnO nanoparticles as annealing temperature increases may be attributed to the defects that are in the ZnO nanoparticles.

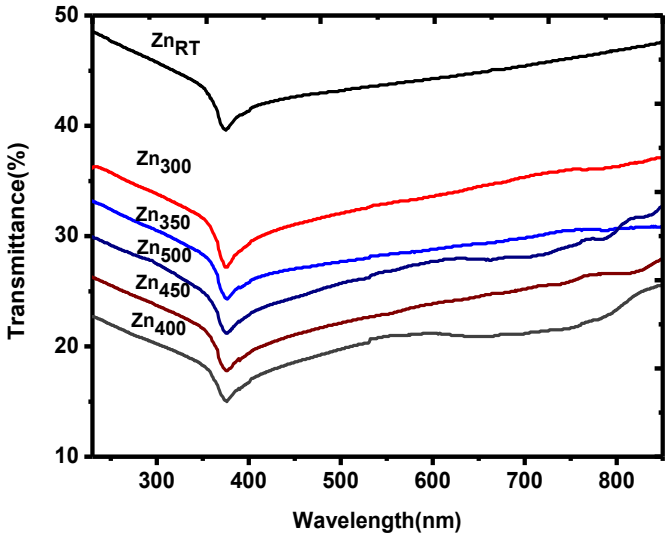

Fig (3): Transmittance spectra of ZnO nanoparticles annealed at different temperatures

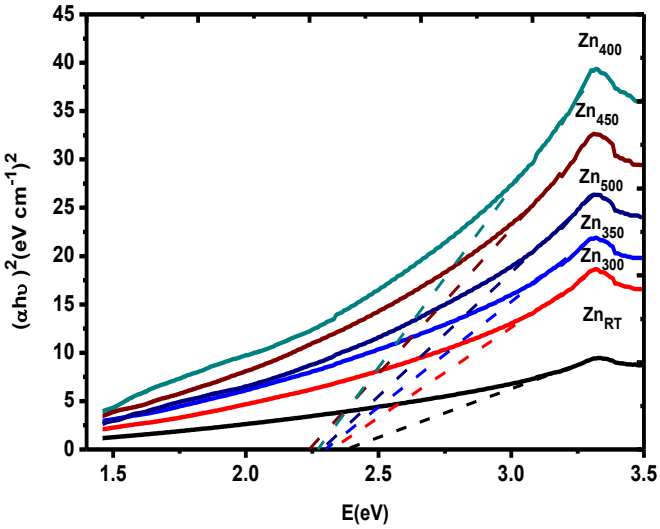

Fig (4): Plot of $(\alpha h\upsilon)^2$ vs. hυ of deposited ZnO nanoparticles annealed at different temperatures.

Table (2): vacancy energy levels and average grain size at different annealing temperatures**.**

Annealing temperature (^{o}C)	vacancy energy levels E_v (eV)	Average grain size(nm)
T	2.37	25.7
300	2.32	34.1
350	2.29	34.2
400	2.27	34.6
450	2.25	36.4
500	2.29	33

Fig. (5) shows the vacancy energy levels and the grain size vs. annealing temperature. According to confinement of quantum theory, the band gap energy of a material decreases with increase in size of the quantum dot [16]. So, as the annealing temperature increases from RT to 450^{o}C the grain size increases from 25.7nm to 36.4nm and the vacancy energy levels decreases from 2.37 eV to 2.25 eV ,respectively, then the grain size decreases from 36.4nm to 33nm and the vacancy energy levels increases from 2.25 eV to 2.29 eV as the annealing temperature increases from 400^{o}C to 500^{o}C, respectively.

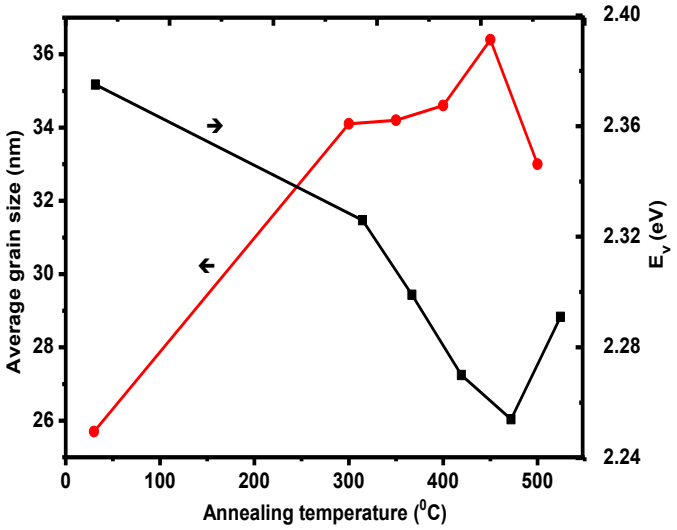

Fig (5): The vacancy energy levels (E_v) and the average grain size of ZnO nanoparticles as a function of annealing temperature.

The extinction coefficient (k) is calculated by the following equation and is shown in Fig (6).

$$k = \frac{\alpha\lambda}{4\pi} \qquad (6)$$

Where λ is the wave length of light and α is the absorption coefficient [15].

One of the significant optical parameter for ZnO thin film is its refractive index. The refractive index (n) can be evaluated due to the following relation and is shown in Fig (7).

$$R = \frac{(n-1)^2+k^2}{(n+1)^2+k^2} \qquad (7)$$

If k $\ll n$ then

$$n = \frac{1+\sqrt{R}}{1-\sqrt{R}} \qquad (8)$$

Where R and k are the reflectance and extinction coefficient of the films, respectively .The complex dielectric constant (ε*) can be obtained by the following relation [15]:

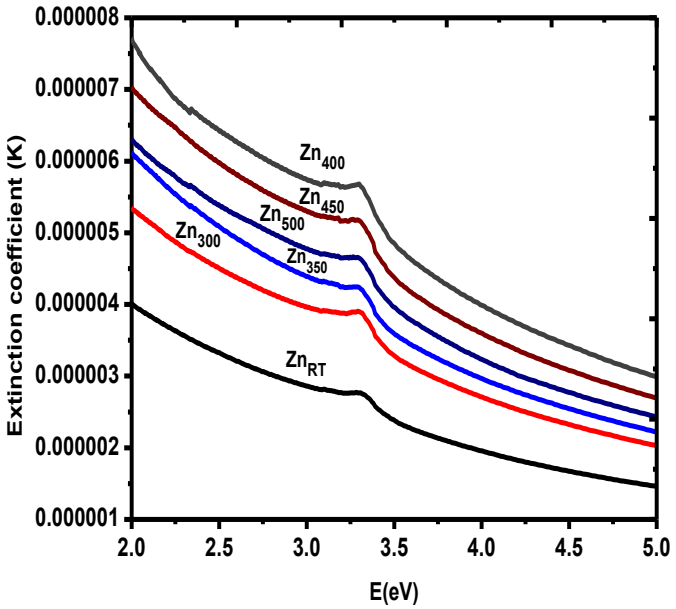

Fig (6): The extinction coefficient of ZnO nanoparticles annealed at different temperatures.

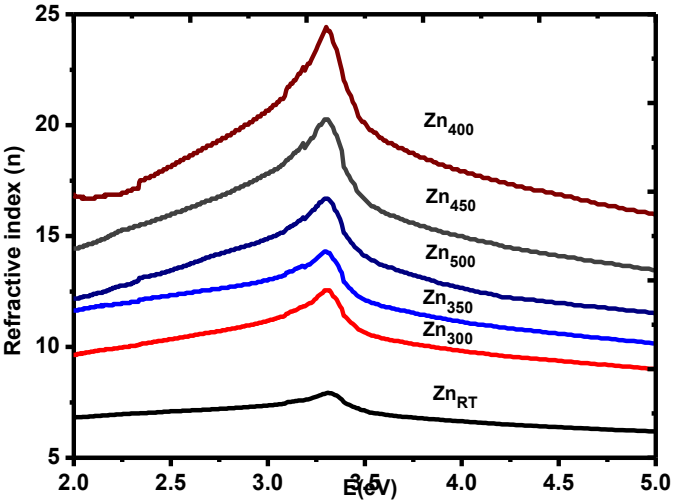

Fig (7): The refractive index of ZnO nanoparticles annealed at different temperatures.

$$\varepsilon^* = \varepsilon_1 - i\varepsilon_2 \quad (9)$$

Where $\varepsilon_1 = n^2 - k^2$ and $\varepsilon_2 = 2nk$ are the real part and the imaginary part of the dielectric constant. The loss factor tan δ is the ratio of ε_2 and ε_1. Fig (8) and Fig (9) shows the real and the imaginary part of complex dielectric constant of ZnO nanoparticles annealed at different temperatures as a function of photon energy.

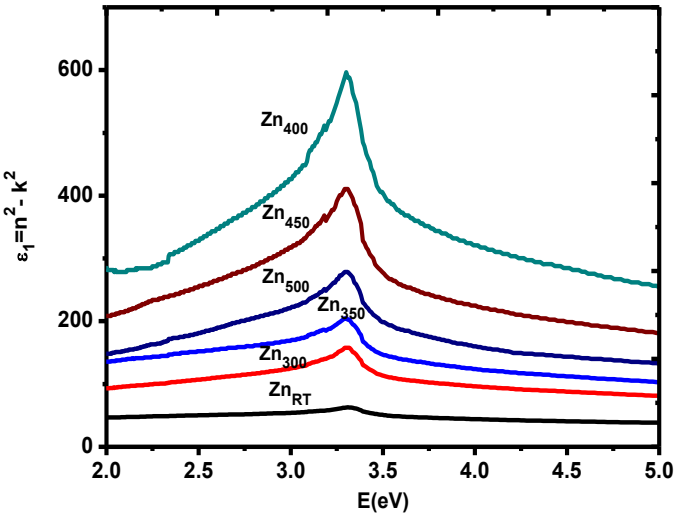

Fig (8): The real part of complex dielectric constant of ZnO nanoparticles annealed at different temperatures

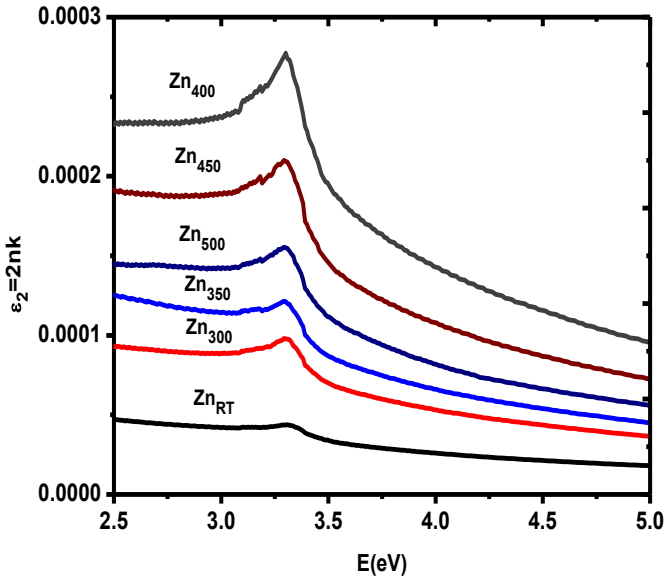

Fig (9): The imaginary part of complex dielectric constant of ZnO nanoparticles annealed at different temperatures.

It well known that as the photon energy increased the absorption inside the ZnO nanoparticles are increased till reach to maximum value; this is due to the electronic transition from valence band to the localized states between valence and conduction bands or to the conduction band. So the values of k, n, ε_1 and ε_2 are increased till reach to maximum value then decreased as shown in Fig (6), Fig (7), Fig (8) and Fig (9).

The values of k, n, ε_1 and ε_2 for the annealed ZnO nanoparticles increase with increasing the annealing temperature. This is due to the increase of average grain size, oxygen vacancies and the carrier concentration with the annealing temperature [17]. The obtained data of n can be further studied to get the high-frequency dielectric constant ε_∞ due to the following process [18]. This process defines the role of the free carriers and the lattice vibration modes of the dispersion. According to Pankove [15].

$$\varepsilon_1 = \varepsilon_\infty - \frac{e^2 N_t}{\pi \varepsilon_o m^* c^2} \lambda^2 \quad (10)$$

Where ε_1 and ε_∞ are the real part and the lattice dielectric constant of the dielectric constant as obtained from Eq. (9), while λ, e, N_t , ε_o, m* and c are the wavelength, the charge of the electron, the free charge-carrier concentration, the permittivity of the free space, the effective mass of the charge carriers in units of kg, and the velocity of light, respectively. It is showed that the dependence of ε_1 on λ^2 is linear at longer wavelengths, as shown in Fig (10). Extrapolating the linear part of this dependence to zero wavelength gives the value of ε_∞ and from the slopes of these lines we can estimate the values of N_t/m^* for the studied nanoparticles. By using eq. (4) we can estimate the free charge-carrier concentration (N_t) then replace the values of (N_t) into the slope to get the effective mass (m*).

The free charge carrier's inter-atomic distance (R) is given by:

$$R = \frac{1}{N_t^{1/3}} \quad (11)$$

The values of ε_∞, N/m*, N_t, m*/m_e and R are tabulated in Table (3).

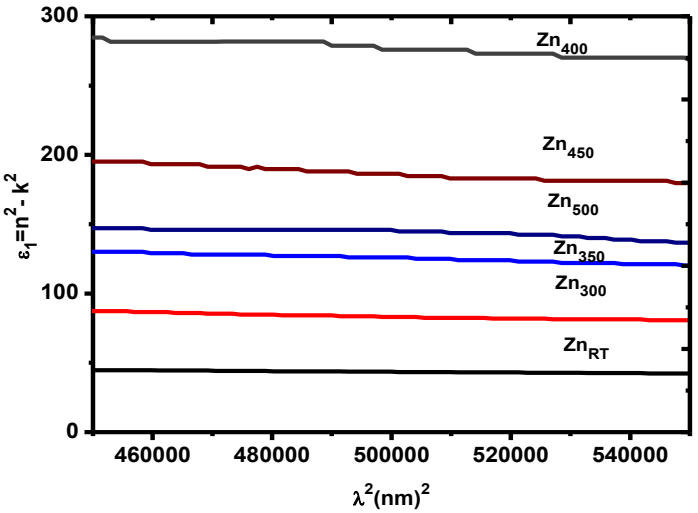

Fig (10): The real part of complex dielectric constant as a function of λ^2 for ZnO nanoparticles annealed at different temperatures.

Table (3): Dielectric constant (ε_∞), N_t/m^*, free charge–carrier concentration (N_t), effective mass of charge carriers (m^*) relative to free electron mass (m_e) and the inter-atomic distance (R) of ZnO nanoparticles at different annealing temperatures.

Annealing temperature (^oC)	ε_∞ ± 0.01	N_t/m^* X10^{56}	N_t (m^{-3}) x10^{28}	m^*/m_e ± 0.1	R(nm) ± 0.01
RT	56	2.45	4.206	18.8	0.2875
300	117	6.62	4.221	6.9	0.2871
350	175	9.7	4.222	4.7	0.2871
400	355	15.47	4.217	2.9	0.2872
450	269	16.2	4.221	2.8	0.2871
500	191	9.27	4.222	4.9	0.2871

3.4. Photoluminescence spectroscopy

PL spectrum of ZnO nanoparticles annealed at different temperatures that excited at 377nm is shown in Fig (11). It is showed that, a strong UV and very weak violet, blue and green emissions are emitted. All the annealed ZnO nanoparticles emit UV, violet, blue and green emissions sited at 392, 420, 484 and 528nm, respectively. The strong UV emission peaks at 392nm are caused from the transfer of electron from conduction band (CB) to valence band (VB) [19].

The violet emission peaks at 420 nm are attributed to the transition of electron from conduction band to zinc vacancies (V_{Zn})[20]. The blue emission peaks at 484 nm are due to the transition of electron from zinc interstitial (Zn_i) to zinc vacancies (V_{Zn})[19]. The green emission peaks at 528 nm are due to the transition of electron from conduction band to the oxygen vacancy defect (V_o) [21]. The annealed ZnO nanoparticles emit strong UV and very weak violet, blue and green emissions this refers to the high crystal quality of annealed ZnO nanoparticles.

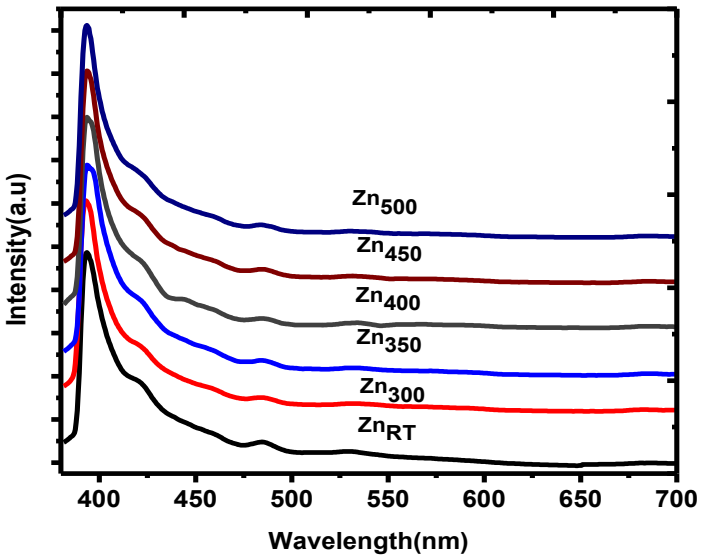

Fig (11): PL spectrum of ZnO nanoparticles annealed at different temperatures.

4. Conclusion

The structural and optical properties of ZnO nanoparticles synthesis by microwave routs were studied. The XRD reveal the presence of hexagonal wurtzite structure of ZnO average grain size 25.7–36.4nm. From the transmission spectra, the vacancy energy level of ZnO was found to be 2.25 - 2.37 eV. The values of k, n, ε_1 and ε_2 for the annealed ZnO nanoparticles increase with increasing the annealing temperature. This is caused by the increase of average grain size, oxygen vacancies and the carrier concentration with the annealing temperature**.** The PL spectra show high crystal quality of annealed ZnO nanoparticles the emission of strong UV and very weak violet, blue and green emissions.

References

[1] Z.L. Wang, Zinc oxide nanostructures: growth, properties and applications, J. Phys.: Condens. Matter 16 (2004) R829–R858.
[2] Z. Fan, J.G. Lu, Zinc oxide nanostructures: synthesis and properties, J. Nanosci. Nanotechnol. 5 (2005) 1561–1573.
[3] P. Yang, H. Yan, S. Mao, R. Russo, J. Johnson, R. Saykally, N. Morris, J. Pham, R.He, H.J. Choi, Controlled growth of ZnO nanowires and their optical properties, Adv. Funct. Mater. 12 (2002) 323–331.
[4] Z. Jia, L. Yue, Y. Zheng, Z. Xu, Rod-like zinc oxide constructed by nanoparticles: synthesis, characterization and optical properties, Mater. Chem. Phys. 107 (2008) 137–141.
[5] B. Li, Y. Wang, Facile synthesis and enhanced photocatalytic performance of flower-like ZnO hierarchical microstructures, J. Phys. Chem. C 114 (2010) 890–896.
[6] W. Jin, I. Lee, A. Kompch, U. Dorfler, M. Wintere, Chemical vapor synthesis and characterization of chromium doped zinc oxide nanoparticles, J. Eur. Ceram. Soc. 27 (2007) 4333–4337.
[7] H. Cheng, J. Cheng, Y. Zhang, Q.M. Wang, Large-scale fabrication of ZnO micro and nano-structures by microwave thermal evaporation deposition, J. Cryst. Growth 299 (2007) 34–40.
[8] H. Wang, J. Z. Xu , J. J. Zhu, and H. Y. Chen . Preparation of CuO nanoparticles by microwave irradiation J. Cryst. Growth, 244 (2002). 88-94
[9] S.Y. Kuo, W.C. Chen, C. P. Cheng, Investigation of annealing-treatment on the optical and electrical properties of sol–gel-derived zinc oxide thin films Superlattices Microstruct. 39 (2006) 162–170.
[10] H.M. Zhou, D.Q. Yi, Z.M. Yu, L.R. Xiao, J. Li, Preparation of aluminum doped zinc oxide films and the study of their

microstructure, electrical and optical properties Thin Solid Films 515 (2007) 6909–6914
[11] C.C. Hsu, N.L. Wu, J. Photocatalytic activity of ZnO/ZnO2 composite, Photochem. Photobiol. A: Chem. 172 (2005) 269–274.
[12] M. M. El-Desoky, M. A. Ali , G. Afifi ,H. Imam, Annealing effects on the structural and optical properties of growth ZnO thin films fabricated by pulsed laser deposition (PLD), J Mater Sci: Mater Electron 25 (11), 507 (2014)1-5077.
[13] M. Tiemann, F. Marlow, J. Hartikainen,O . Weiss, M. Linder, Ripening effects in ZnS nanoparticle growth, J. Phys. Chem. C 112 (2008) 1463–1467.
[14] Zhu BL, Sun XH, Zhao XZ, Su FH, Li GH, Wu XG, et al. The effects of substrate temperature on the structure and properties of ZnO films prepared by pulsed laser deposition. Vacuum 2008;82:495–500.
[15] I. Pankove. Optical processes in semiconductors. New Jersey: Prentice-Hall Inc.; 1971.
[16] Y.G. Wang, S.P. Lau, H.W. Lee, S.F. Yu, S.K. Tay, X.Z. Zang, H.H. Hing, J. Appl. Phys. 94 (2003) 354.
[17] A.I. Ali , A.H. Ammar, A. Abdel Moez**,** Influence of substrate temperature on structural, optical properties and dielectric results of nano- ZnO thin films prepared by Radio Frequency technique, Superlattices and Microstructures 65 (2014) 285–298.
[18] M.M. El- Desoky.Characterization and transport properties of V_2O_5–Fe_2O_3–TeO_2 glasses ,J. Non-Cryst Solids 351(2005) 3139-3146
[19] X.Q. Wei, Z. Zhang, Y.X. Yu , B.Y. Man. Comparative study on structural and optical properties of ZnO thin films prepared by PLD using ZnO powder target and ceramic target. Optics, Laser Technology 41 (2009) 530–534.
[20] Tapas Kumar Kundu, Nantu Karak , Puspendu Barik , Satyajit Saha. Optical Properties of Zno Nanoparticles Prepared by Chemical Method Using Poly (VinylAlcohol) (PVA) as Capping Agent. International Journal of Soft Computing and Engineering (IJSCE) ISSN: 2231-2307, Volume-1, Issue-NCRAMT2011, July 2011.
[21]Jinghai Yang, Xiaoyan Liu, Lili Yang, Yaxin Wang, Yongjun Zhang, Jihui Lang, Ming Gao, Maobin Wei, Effect of different annealing atmospheres on the structure and optical propertiesof ZnO nanoparticles, Journal of Alloys and Compounds 485 (2009) 743–746.